

Research



Cite this article: Colbrook MJ, Ayton LJ, Fokas AS. 2019 The unified transform for mixed boundary condition problems in unbounded domains. *Proc. R. Soc. A* **475**: 20180605. <http://dx.doi.org/10.1098/rspa.2018.0605>

Received: 3 September 2018

Accepted: 10 January 2019

Subject Areas:

applied mathematics, differential equations

Keywords:

analytical methods, Wiener–Hopf, unified transform, mixed boundary conditions

Authors for correspondence:

Matthew J. Colbrook

e-mail: m.colbrook@damtp.cam.ac.uk

Lorna J. Ayton

e-mail: l.j.ayton@damtp.cam.ac.uk

Electronic supplementary material is available online at <https://doi.org/10.6084/m9.figshare.c.4381772>.

The unified transform for mixed boundary condition problems in unbounded domains

Matthew J. Colbrook, Lorna J. Ayton and
Athanasios S. Fokas

Department of Applied Mathematics and Theoretical Physics,
University of Cambridge, Wilberforce Road, Cambridge CB3 0WA, UK

MJC, 0000-0003-4964-9575; LJA, 0000-0001-6280-9460

This paper implements the unified transform to problems in unbounded domains with solutions having corner singularities. Consequently, a wide variety of mixed boundary condition problems can be solved without the need for the Wiener–Hopf technique. Such problems arise frequently in acoustic scattering or in the calculation of electric fields in geometries involving finite and/or multiple plates. The new approach constructs a global relation that relates known boundary data, such as the scattered normal velocity on a rigid plate, to unknown boundary values, such as the jump in pressure upstream of the plate. By approximating the known data and the unknown boundary values by suitable functions and evaluating the global relation at collocation points, one can accurately obtain the expansion coefficients of the unknown boundary values. The method is illustrated for the modified Helmholtz and Helmholtz equations. In each case, comparisons between the traditional Wiener–Hopf approach, other spectral or boundary methods and the unified transform approach are discussed.

1. Introduction

Mixed boundary condition problems arise in a number of physical situations, for example, in the scattering of sound by a rigid plate, which is governed by the Helmholtz equation. In this case, the boundary conditions change suddenly from a zero-normal velocity condition on the rigid surface to a suitable continuity

condition across the upstream and downstream zero-streamline. In the field of electrical engineering, mixed boundary conditions can also arise in the modelling of the flow of electrorheological fluids when exposed to long electrodes [1]. This situation is governed by the Laplace equation and the boundary conditions change from the known electric potential on the electrodes to a known jump in derivatives of the electric potential.

If there is only one point at which the type of condition changes, these mixed boundary condition problems can be solved, often exactly, by applying the Wiener–Hopf method [2]. Such a well-known one-point problem arises from the scattering of a sound wave by a semi-infinite flat plate, also known as the Sommerfeld diffraction problem [3]. The Wiener–Hopf method is effective in this case because a single scalar kernel function, $\kappa(\lambda)$, is required to be factorized as $\kappa(\lambda) = \kappa_-(\lambda)\kappa_+(\lambda)$, where $\kappa_{\pm}(\lambda)$ is analytic in the upper/lower half of the complex λ plane, respectively. For a scalar function, one can typically obtain a suitable factorization via the use of the Cauchy integral formula [2].

When a sudden change of boundary condition occurs in more than one location, such as in the case of sound scattering by two semi-infinite staggered plates [4], the Wiener–Hopf method gives rise to a matrix equation. The Wiener–Hopf factorization of a matrix, $M(\lambda)$, involves obtaining two matrices, $M_{\pm}(\lambda)$ which are analytic in the upper/lower half of the complex λ plane, respectively, such that $M_-M_+ = M$. However, unlike the commutative scalar case, for a general matrix, there is no formula equivalent to the Cauchy integral formula that allows one to obtain a suitable matrix factorization. Only matrices of very specific forms are known to be factorizable exactly [5]. To illustrate the difficulty of matrix Wiener–Hopf problems, consider the semi-infinite staggered plates of [4] which have endpoints $(0, -h)$ and $(-a, 0)$. The matrix arising from the Wiener–Hopf analysis is given by

$$\begin{pmatrix} 1 & e^{ia\lambda - h\gamma(\lambda)} \\ e^{-ia\lambda - h\gamma(\lambda)} & 1 \end{pmatrix}, \quad (1.1)$$

where $\gamma(\lambda) = \sqrt{\lambda^2 - k_0^2}$ and k_0 is the reduced frequency of the incident sound wave being scattered by the plates. This is a particularly difficult matrix to factorize due to the existence of the factors $e^{\pm ia\lambda}$ which grow exponentially in the lower/upper halves of the complex λ plane as $|\lambda| \rightarrow \infty$. Having such exponential growth prohibits the use of Liouville’s theorem which is vital for progress in the Wiener–Hopf method. To deal with these exponential factors, an ingenious but lengthy procedure is implemented in [4], which unfortunately cannot be extended to general matrices with exponential factors. Therefore, upon finding a matrix with such exponential factors, it is not clear if, in fact, it can be factorized. Indeed, a similarly structured matrix arises for sound scattering by a semi-infinite impermeable plate with a finite permeable extension [6], and in this case, an iterative procedure is implemented to obtain the approximate solution.

As many relevant physical problems consist of interactions with more than one point of sudden change of boundary conditions (relating to finite structures), it is imperative to have efficient and reliable methods to tackle these multi-point problems. In this paper, we discuss an alternative approach to mixed boundary condition problems that does not involve the Wiener–Hopf method. This approach is based on the unified transform [7], commonly known as the Fokas method, which employs the so-called global relation. The analysis of the global relation, which relates appropriate transforms of the given boundary data with transforms of the unknown boundary values, provides a mathematically elegant and also computationally efficient characterization of the general Dirichlet to Neumann (DtN) map, [8]. A previous approach using the unified transform to avoid Wiener–Hopf factorization can be found in [9] and has been seen to work for two-point problems. This different approach, for the harmonic and biharmonic equations, requires analysis of the zeros of functions arising in the global relation.

Recently, a simple and efficient technique based on the unified transform has been introduced [10] for the numerical evaluation of the approximate global relation for the case of a bounded polygonal domain. This involves approximating the given data and the unknown boundary values in terms of expansions of suitable basis functions, and then determining the expansion

coefficients by evaluating the approximate global relation at a set of discrete values of λ , called collocation points. To tackle problems which involve unbounded domains (formed by the exterior of one or more finite or semi-infinite infinitesimally thin strips in \mathbb{R}^2), we will present a modification of the above procedure of evaluating the DtN map. Furthermore, we discuss at length suitable basis functions and collocation points to obtain spectral accuracy in the presence of singularities encountered in typical problems. After the DtN map has been computed, all boundary values are known and the solution can be computed using either the solution formulae obtained via the unified transform or the classical representations involving the associated fundamental solutions [11]. The ability to calculate all boundary values quickly and efficiently is particularly advantageous for acoustics, as a simple application of the Ffowcs Williams–Hawkings technique [12] allows one to obtain far-field noise from boundary pressure data. Our results can also be extended to more general scattering/exterior problems.

This paper is organized as follows: In §2, we review the DtN map for the modified Helmholtz, Helmholtz, and for completeness, Laplace, equations in a bounded polygonal domain. We also discuss how to adapt the method in the case of unbounded domains. In §3, we illustrate the DtN map for the modified Helmholtz and Helmholtz equations, extending the earlier analysis to the case of semi-infinite domains. Specifically, in §3a, we use the unified transform to derive the DtN map for a semi-infinite flat plate problem governed by the modified Helmholtz equation and compare the approximate solution against the known exact solution found analytically via the traditional Wiener–Hopf technique [2]. In §3b, we illustrate the Helmholtz equation for a four-point problem by considering acoustic scattering by two finite parallel staggered plates; the traditional Wiener–Hopf approach yields a 4×4 matrix which cannot be factorized easily, whereas the unified transform allows us to approximate the surface response quickly and efficiently. The method is found to be competitive with spectral and boundary integral methods. Our conclusions are summarized in §4.

2. The unified transform method

Here, we discuss the use of the unified transform for solving the Helmholtz, modified Helmholtz and Laplace equations,

$$\frac{\partial^2 q}{\partial x^2} + \frac{\partial^2 q}{\partial y^2} + k_0^2 q = 0, \quad \frac{\partial^2 q}{\partial x^2} + \frac{\partial^2 q}{\partial y^2} - k_0^2 q = 0 \quad \text{and} \quad \frac{\partial^2 q}{\partial x^2} + \frac{\partial^2 q}{\partial y^2} = 0, \quad (2.1)$$

in the interior of a convex polygonal domain, \mathcal{D} , with boundary $\partial\mathcal{D}$, as discussed in [7].

To derive the global relation for the Helmholtz equation, let v be a solution to its adjoint (also the Helmholtz equation). Multiplying the Helmholtz equation by v , and then subtracting the same equation with q and v interchanged, we find

$$\frac{\partial}{\partial x} \left(v \frac{\partial q}{\partial x} - q \frac{\partial v}{\partial x} \right) + \frac{\partial}{\partial y} \left(v \frac{\partial q}{\partial y} - q \frac{\partial v}{\partial y} \right) = 0. \quad (2.2)$$

Then, Green's theorem implies

$$\int_{\partial\mathcal{D}} \left[\left(v \frac{\partial q}{\partial x} - q \frac{\partial v}{\partial x} \right) dy - \left(v \frac{\partial q}{\partial y} - q \frac{\partial v}{\partial y} \right) dx \right] = 0. \quad (2.3)$$

To express the integrand of the above equation in terms of just the Dirichlet and Neumann boundary values, we parametrize $q(x, y)$ and $v(x, y)$ in terms of the arc length, s , of $\partial\mathcal{D}$. Differentiating the function $q(x(s), y(s))$ with respect to s , we find

$$\frac{\partial q}{\partial x} dx + \frac{\partial q}{\partial y} dy = q_T ds, \quad (2.4)$$

where q_T denotes the derivative of q along the tangential direction. Thus,

$$\frac{\partial q}{\partial x} dy - \frac{\partial q}{\partial y} dx = q_n ds, \quad (2.5)$$

where q_n denotes the derivative of q along the outward normal to the boundary. Inserting (2.5) into (2.3) we find the global relation

$$\int_{\partial\mathcal{D}} \left(v \frac{\partial q}{\partial n} - q \frac{\partial v}{\partial n} \right) ds = 0, \quad (2.6)$$

where v is any solution to the (adjoint) Helmholtz equation. Equation (2.6) is also valid for the Laplace equation upon setting $k_0 = 0$, and the modified Helmholtz equation upon $k_0 \rightarrow ik_0$.

In what follows, to further simplify the global relation, we introduce the complex variable $z = x + iy$, and its conjugate $\bar{z} = x - iy$. This enables us to write the Helmholtz, modified Helmholtz and Laplace equations, respectively, in the form

$$\frac{\partial^2 q}{\partial z \partial \bar{z}} + \beta^2 q = 0, \quad \frac{\partial^2 q}{\partial z \partial \bar{z}} - \beta^2 q = 0, \quad \frac{\partial^2 q}{\partial z \partial \bar{z}} = 0, \quad (2.7)$$

where $\beta = k_0/2$.

We choose the following particular solutions of the Helmholtz, modified Helmholtz and Laplace equations:

$$v = e^{-i\beta(\lambda z + \bar{z}/\lambda)}, \quad v = e^{-i\beta(\lambda z - \bar{z}/\lambda)}, \quad v = e^{-i\lambda z}. \quad (2.8)$$

Then, (2.6) gives for Helmholtz the global relation

$$\int_{\partial\mathcal{D}} e^{-i\beta(\lambda z + \bar{z}/\lambda)} \left[q_n + \beta \left(\lambda \frac{dz}{ds} - \frac{1}{\lambda} \frac{d\bar{z}}{ds} \right) q \right] ds = 0, \quad \lambda \in \mathbb{C} \setminus \{0\}, \quad (2.9)$$

for modified Helmholtz, we find

$$\int_{\partial\mathcal{D}} e^{-i\beta(\lambda z - \bar{z}/\lambda)} \left[q_n + \beta \left(\lambda \frac{dz}{ds} + \frac{1}{\lambda} \frac{d\bar{z}}{ds} \right) q \right] ds = 0, \quad \lambda \in \mathbb{C} \setminus \{0\} \quad (2.10)$$

and for Laplace,

$$\int_{\partial\mathcal{D}} e^{-i\lambda z} \left[q_n + \lambda \frac{dz}{ds} q \right] ds = 0, \quad \lambda \in \mathbb{C}. \quad (2.11)$$

Equations (2.9)–(2.11) involve only q and its normal derivative, q_n , on the boundary. Note also that these three cases deal with more general second-order elliptic constant coefficient PDEs through a suitable linear change of variables.

The range of values of the complex parameter λ for which the global relations are valid depends on the domain \mathcal{D} . If the domain is bounded, the global relations are valid for all complex λ (excluding 0 for Helmholtz/modified Helmholtz), as each integral along the boundary always converges. If the domain is semi-infinite or infinite, then the range of values of λ for which the integrals converge are limited by enforcing convergence within the whole domain to ensure the validity of Green's theorem. In particular, $\text{Re}[-i\beta(\lambda z + \bar{z}/\lambda)] < 0$ for Helmholtz, $\text{Re}[-i\beta(\lambda z - \bar{z}/\lambda)] < 0$ for modified Helmholtz and $\text{Re}[-i\lambda z] < 0$ for Laplace. Other values can also be included by assuming q satisfies certain conditions at infinity (see [13]).

(a) Dirichlet to Neumann map

The DtN map is discussed in [10] for finite polygonal domains; we review the relevant details here for the Helmholtz, modified Helmholtz and Laplace equations.

Let $\partial\mathcal{D}$ consists of M straight sides such that \mathcal{D} is a convex M -gon (for extensions to non-convex polygons, we refer the reader to [14]). The unified transform can also be used for circular domains [15–17] and domains with general curved edges [18]). Let q^j and q_n^j denote the Dirichlet

and Neumann boundary values on the j^{th} side which connects corners z_j and z_{j+1} . We expand q^j and q_n^j in terms of a collection of basis functions, $S_n(t)$:

$$q^j(t) \approx \sum_{n=0}^{N-1} a_n^j S_n(t), \quad q_n^j(t) \approx \sum_{n=0}^{N-1} b_n^j S_n(t), \quad (2.12)$$

where $t \in [-1, 1]$ provides a suitable parametrization of $\partial\mathcal{D}$. Such a parametrization is given in [10] by considering the j^{th} side of the polygon:

$$z = m_j + th_j, \quad m_j = \frac{1}{2}(z_j + z_{j+1}), \quad h_j = \frac{1}{2}(z_{j+1} - z_j). \quad (2.13)$$

Substituting the function expansions into the global relation for Helmholtz, (2.9), yields

$$\sum_{j=1}^M \sum_{n=0}^{N-1} e^{-i\beta(\bar{m}_j/\lambda + \lambda m_j)} \left[b_n^j |h_j| + a_n^j \beta \left(\lambda h_j - \frac{\bar{h}_j}{\lambda} \right) \right] \hat{S}_n \left[i\beta \left(\frac{\bar{h}_j}{\lambda} + \lambda h_j \right) \right] = 0, \quad (2.14)$$

for $\lambda \in \mathbb{C} \setminus \{0\}$, where

$$\hat{S}_n(\lambda) = \int_{-1}^1 e^{i\lambda t} S_n(t) dt, \quad \lambda \in \mathbb{C}, \quad (2.15)$$

which is consistent with [10]. Similarly, modified Helmholtz, (2.10), yields

$$\sum_{j=1}^M \sum_{n=0}^{N-1} e^{i\beta(\bar{m}_j/\lambda - \lambda m_j)} \left[b_n^j |h_j| + a_n^j \beta \left(\lambda h_j + \frac{\bar{h}_j}{\lambda} \right) \right] \hat{S}_n \left[-i\beta \left(\frac{\bar{h}_j}{\lambda} - \lambda h_j \right) \right] = 0, \quad (2.16)$$

for $\lambda \in \mathbb{C} \setminus \{0\}$, and for Laplace, (2.11), we obtain

$$\sum_{j=1}^M \sum_{n=0}^{N-1} e^{-im_j \lambda} \left[b_n^j |h_j| + a_n^j \lambda h_j \right] \hat{S}_n [i\lambda h_j] = 0, \quad \lambda \in \mathbb{C}. \quad (2.17)$$

For any given boundary value problem, some of the constants $\{a_j, b_j\}$ are known, and some unknown. By evaluating the approximate global relation, (2.14) and its Schwartz conjugate (which is given by taking the complex conjugate then replacing λ with $\bar{\lambda}$) if the solution is real, at suitably chosen Fourier collocation points, $\lambda_i \in \mathbb{C}$, we can construct sufficiently many equations for the unknown constants $\{a_j, b_j\}$. Discussion of how optimal collocation points are chosen for bounded domains can be found in [10,19].

(b) Extension to semi-infinite domains

We can extend the earlier construction in the case of a semi-infinite convex polygonal domain (such as the upper half plane) by imposing a suitable decay condition, such as a radiation condition, on the solution q as $|z| \rightarrow \infty$, so that all required integrals converge. The global relations, (2.9), (2.10) and (2.11), remain valid; however, rather than using the parametrization $t \in [-1, 1]$, in the case of infinite edges, we need to use a parametrization $t \in [0, \infty)$ or $t \in (-\infty, \infty)$. We therefore require relevant basis functions over semi-infinite domains which also capture the appropriate decay at infinity.

Also, as stated earlier, the λ -domain over which the global relations, (2.9), (2.10) or (2.11), hold must now be restricted. As \mathcal{D} is semi-infinite, λ is restricted to a subset of the complex plane. Thus, rather than applying the Schwartz conjugate to the global relation, we may need to find another suitable symmetry (which will be discussed within each example below).

3. Examples and results

We now present examples of the global relation for the modified Helmholtz and Helmholtz equations. First, in §3a, we use the global relation (2.10) for the modified Helmholtz equation to obtain the approximate solution to a semi-infinite half-plate problem. In §3b, we use the global

relation to solve the Helmholtz equation for the scattering of a (complex) plane wave by two finite staggered plates, a situation which gives rise to a 4×4 matrix Wiener–Hopf problem.

These examples illustrate the effectiveness of the new approximate global relation method for determining the solution to elliptic PDEs in semi-infinite polygonal domains that have been so far solved via the Wiener–Hopf method. We also compare the new approach to boundary integral and spectral methods. All numerical experiments were run on a 1.80 GHz processor in Matlab. Code for the examples can be found at <http://www.damtp.cam.ac.uk/user/mjc249/code.html>.

(a) Modified Helmholtz: semi-infinite half plate

We consider the following problem

$$\frac{\partial^2 q}{\partial x^2} + \frac{\partial^2 q}{\partial y^2} - k_0^2 q = 0, \quad (3.1)$$

subject to

$$\frac{\partial q}{\partial y}(x, 0_{\pm}) = f(x), \quad x > 0, \quad [q](x, 0) = [q_y](x, 0) = 0, \quad x < 0, \quad (3.2)$$

where $[q](x, y_0)$ denotes the jump in q across $y = y_0$. For this example, we choose, $f(x) = e^{-x/2}$ (lengths scaled with k_0^{-1}) to ensure the Wiener–Hopf equation can be factorized exactly without the need for the (numerical) Cauchy integral formula (this is not always the case with more complicated boundary conditions).

The Wiener–Hopf solution [2] of the above boundary value problem is given by

$$q(x, y) = \frac{\text{sgn}(y)}{2\pi\sqrt{i(k_0 + 1/2)}} \int_{-\infty}^{\infty} \frac{e^{-i\lambda x - |y|\sqrt{\lambda^2 + k_0^2}}}{(\lambda + i/2)\sqrt{\lambda + ik_0}} d\lambda. \quad (3.3)$$

(i) Global relation

To obtain a suitable global relation, we consider (2.10) applied over the following two domains,

$$\mathcal{S}_1 = \{-\infty < x < \infty, 0_+ \leq y < \infty\}, \quad \mathcal{S}_2 = \{-\infty < x < \infty, -\infty < y \leq 0_-\}. \quad (3.4)$$

Then (2.10) yields the following equation:

$$\int_{-\infty}^0 e^{-i\beta x(\lambda - 1/\lambda)} \left(-\frac{\partial q}{\partial y}(x, 0_+) + \beta \left(\lambda + \frac{1}{\lambda} \right) q(x, 0_+) \right) dx + \int_0^{\infty} e^{-i\beta x(\lambda - 1/\lambda)} \left(-f(x) + \beta \left(\lambda + \frac{1}{\lambda} \right) q(x, 0_+) \right) dx = 0, \quad \lambda \in \mathbb{R}_-, \quad (3.5)$$

together with

$$\int_{-\infty}^0 e^{-i\beta x(\lambda - 1/\lambda)} \left(\frac{\partial q}{\partial y}(x, 0_-) - \beta \left(\lambda + \frac{1}{\lambda} \right) q(x, 0_-) \right) dx + \int_0^{\infty} e^{-i\beta x(\lambda - 1/\lambda)} \left(f(x) - \beta \left(\lambda + \frac{1}{\lambda} \right) q(x, 0_-) \right) dx = 0, \quad \lambda \in \mathbb{R}_+, \quad (3.6)$$

where $\beta = k_0/2$. A suitable symmetry transform in this case consists of taking the complex conjugate and then replacing λ by $-\lambda$. We take this symmetry transform of (3.6) and then subtract the resulting equation from (3.5):

$$\int_{-\infty}^0 e^{-i\beta x(\lambda - 1/\lambda)} \frac{\partial q}{\partial y}(x, 0) dx - \int_0^{\infty} e^{-i\beta x(\lambda - 1/\lambda)} \frac{\beta}{2} \left(\lambda + \frac{1}{\lambda} \right) [q](x, 0) dx = - \int_0^{\infty} e^{-i\beta x(\lambda - 1/\lambda)} f(x) dx = \frac{2i}{2\beta(\lambda - 1/\lambda) - i}, \quad \lambda \in \mathbb{R}_-. \quad (3.7)$$

Suppose we expand the unknown functions as follows:

$$q_y(-x, 0) = \sum_{n=0}^{N_1-1} a_n S_{n,1}(x), \quad x > 0 \quad (3.8)$$

and

$$[q](x, 0) := q(x, 0_+) - q(x, 0_-) = \sum_{n=0}^{N_2-1} b_n S_{n,2}(x), \quad x > 0, \quad (3.9)$$

where the constants a_n, b_n are to be determined and $\{S_{n,j}\}_{n \geq 0}$ are suitable collections of expansion functions. Substituting (3.8) and (3.9) yields the global relation

$$\sum_{n=0}^{N_1-1} a_n \hat{S}_{n,1} \left[\beta \left(\lambda - \frac{1}{\lambda} \right) \right] - \sum_{n=0}^{N_2-1} b_n \frac{\beta}{2} \left(\lambda + \frac{1}{\lambda} \right) \hat{S}_{n,2} \left[-\beta \left(\lambda - \frac{1}{\lambda} \right) \right] = \frac{2i}{2\beta(\lambda - 1/\lambda) - i}, \quad (3.10)$$

where

$$\hat{S}_{n,j}(\lambda) = \int_0^\infty S_{n,j}(x) e^{i\lambda x} dx. \quad (3.11)$$

By evaluating (3.10) at appropriate collocation points λ_i , we can solve for the unknown constants a_i, b_i via a linear system of equations. Typically, we overdetermine the system and then solve in the least squares sense. If the full solution is needed, it can be computed using the computed unknown $[q](x, 0)$ and the given data $f(x)$ via Green's representation formula.

(ii) Choices of basis functions and singularities

A suitable choice of basis functions is determined from the regularity of the solution. For example, if the unknown boundary values are smooth (and decay sufficiently rapidly), then experimentation suggests $\{L_n(x) e^{-x/2}\}_{n \geq 0}$ are suitable, where L_n denotes the standard Laguerre polynomials. However, for solutions with singular behaviour, it is important to choose basis functions that incorporate these singularities to gain rapid convergence. This is discussed in the context of the unified transform (for *bounded* domains) in [14,20] and a survey of how to deal with singularities in the wider PDE literature can be found in [21].

In this example, the behaviour of the solution at the origin is typically singular and is of fundamental concern during the Wiener–Hopf method as it is used during the Wiener–Hopf analysis when invoking Liouville's theorem to bound the large behaviour of formally unknown functions and determine the associated needed entire function. In addition, the edge behaviour ensures the Wiener–Hopf solution is unique (a full discussion of edge behaviour for Wiener–Hopf problems can be found in [2, §2]).

It is well known that the singular behaviour can be predicted from the geometry of the domain [22–24]. In our case, the solution is odd in the y variable and hence the problem is equivalent to the modified Helmholtz equation in the upper half plane with the given Neumann boundary condition along $x > 0$ and homogeneous Dirichlet boundary condition along $x < 0$. Locally around the origin, this gives the following functions in polar coordinates:

$$I_{n-1/2}(k_0 r) \cos[(n - \frac{1}{2})\theta], \quad n \in \mathbb{N}, \quad (3.12)$$

where I_m are modified Bessel functions of the first kind. Hence $q(x, 0)$ has \sqrt{x} type behaviour as $x \downarrow 0$ and $q_y(-x, 0)$ has a $1/\sqrt{x}$ type singularity as $x \downarrow 0$. A good choice of basis functions should satisfy two criteria; first, it should capture such algebraic behaviours (as well as the relevant

decay at infinity) and second it should have an easily computed Laplace/Fourier transform. The generalized Laguerre polynomials for $\alpha > -1$ have the explicit expansion

$$L_n^\alpha(x) = \sum_{j=0}^n (-1)^j \binom{n+\alpha}{n-j} \frac{x^j}{j!}. \quad (3.13)$$

Selecting basis functions as $x^\alpha L_n^\alpha(x)$ with $\alpha = -1/2$ thus provides the relevant square-root behaviour of interest. These are particularly useful as a straightforward calculation yields

$$\int_0^\infty x^\alpha L_n^\alpha(x) e^{-x/2} e^{i\lambda x} dx = \frac{\Gamma(\alpha)}{B(n+1, \alpha)} \left(1 - \frac{1}{1/2 - i\lambda}\right)^n \left(\frac{1}{2} - i\lambda\right)^{-(\alpha+1)}, \quad (3.14)$$

where B denotes the Beta function. This can be efficiently evaluated, as can the generalized Laguerre polynomials using their recurrence relations, allowing us to both approximate the global relation and reconstruct the approximate solution.

(iii) Choice of collocation points

For the majority of spectral collocation methods, there is a standard theory that describes the best positions of collocation points due to the link with interpolation [25]. However, there is no general theory on the optimum choice of collocation points for the unified transform due to the fact that collocation happens in Fourier space. Instead, there are only simple heuristics. One notable example is the choice found in [10] that leads to block diagonally dominant linear systems for *convex* polygons. No such choice is possible here due to the restriction $\lambda \in \mathbb{R}_-$. Instead, we choose collocation points somewhat randomly. Choosing true random points is a bad strategy as dense clusters will occasionally form which can lead to ill-conditioned linear systems. Thus, we follow [20] and select Halton nodes which create scattered points with a lack of regularity and can be easily generated in MATLAB. These are examples of a quasi-random number sequence and are used in the theory of numerical integration [26] (for example, the one-dimensional sequence using base two has n th number as the number n written in binary and suitably inverted). The idea is that for a suitably large number of such collocation points, the linear system we solve becomes well conditioned. For our problem, we have found that a good choice is to take M Halton nodes inside the interval $[-1, 0)$. As we shall see later, this can be interpreted as sampling the Fourier transform of the boundary integral equations for frequencies in the interval $(-\infty, 0]$. The symmetry transform then implies sampling along the positive axis $[0, \infty)$ as well. It is well known that the singularities of a function are determined by the large wavenumber asymptotics of its Fourier transform and we found that sampling large frequencies was necessary to obtain the most accurate results.

(iv) Numerical performance

In this section, we choose $k_0 = 3$. Larger frequencies will be discussed later. We will compare the approximate solution obtained by the unified transform to the analytic values. These can be found from (3.3) and some simple integral evaluations:

$$\frac{[q](x, 0)}{2} = q(x, 0_+) = -\frac{e^{-x/2}}{\sqrt{k_0^2 - 1/4}} \operatorname{erf}\left(\sqrt{\left(k_0 - \frac{1}{2}\right)x}\right), \quad x \in \mathbb{R}_+ \quad (3.15)$$

and

$$q_y(-x, 0) = \frac{-e^{-k_0 x}}{\sqrt{\pi(k_0 + 1/2)x}} + e^{x/2} \operatorname{erfc}\left(\sqrt{\left(k_0 + \frac{1}{2}\right)x}\right), \quad x \in \mathbb{R}_+. \quad (3.16)$$

Note in particular, there are two different scales of exponential decay; $\exp(-x/2)$ for the unknown Dirichlet values, and $\exp(-k_0 x)$ for the unknown Neumann values. We will see later that these two scales can make it difficult to apply standard spectral methods which typically expand q over the whole domain.

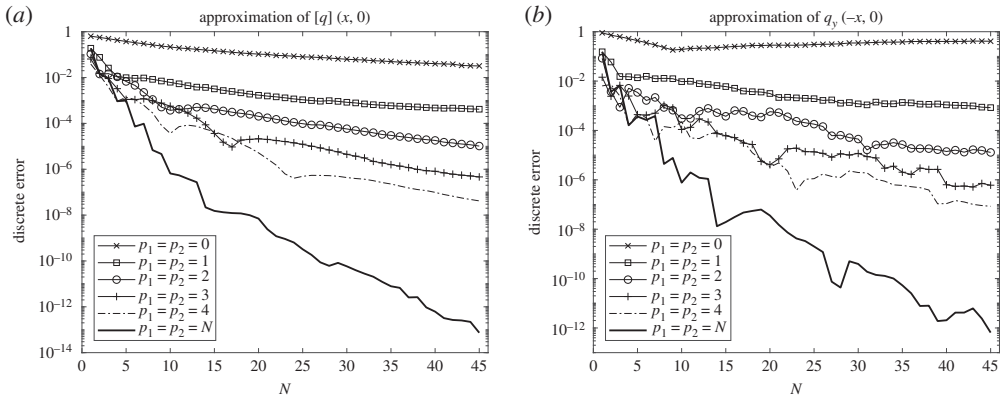


Figure 1. (a) Convergence of computed Dirichlet jump values along the positive axis. (b) Convergence of computed Neumann values along the negative axis.

For the unknown Dirichlet values $[q](x, 0)$, we choose basis functions

$$\{L_n(l_1x)e^{-l_1x/2}\}_{n=0}^{N-1} \cup \left\{ \sqrt{l_1x}L_n^{1/2}(l_1x)e^{-l_1x/2} \right\}_{n=0}^{p_1-1},$$

and for the unknown Neumann values $q_y(-x, 0)$ we choose basis functions

$$\{L_n(l_2x)e^{-l_2x/2}\}_{n=0}^{N-1} \cup \left\{ \frac{L_n^{-1/2}(l_2x)}{\sqrt{l_2x}} e^{-l_2x/2} \right\}_{n=0}^{p_2-1}.$$

The idea is that we can adjust p_1 and p_2 to capture the singularities of the unknown boundary values. The problem with using (3.12) directly is that these Bessel functions diverge at infinity. The extra scaling parameters l_1, l_2 appear due to the fact that the intervals are of infinite length. Such scaling is common in spectral methods and can effect convergence results [27,28]. We took $l_1 = 1$ and $l_2 = 2k_0$. Note that these can be chosen without knowing the analytic solution—the given Neumann data suggest $l_1 = 1$, whereas asymptotics for radial solutions of the modified Helmholtz equation suggest $l_2 = 2k_0$. For medium k_0 , we found this not to be important, but it was important when k_0 is large. Our basis is over-complete, meaning we can obtain expansions after removing some of the basis functions (e.g. $p_1 = p_2 = 0$). However, we found this was useful in gaining accurate solutions that capture the singularities. Many successful (pseudo-)spectral methods also employ such expansions or even do not have a well-defined basis at all [29].

We have measured a discrete error by measuring the maximum error over the evenly spaced points $0.01, 0.02, \dots, 10$ for $[q](x, 0)$ and $0.01, 0.02, \dots, 1$ for $q_y(-x, 0)$, in each case dividing by the maximum value of the true solution over these points to gain a relative error. We took $M = 6 \cdot (2N + p_1 + p_2)$ collocation points (a much smaller number produced similar results but even with the above choice the method was very fast). Figure 1 shows the convergence of the unified transform for different N, p_1 and p_2 . As expected, for fixed p_1, p_2 , we gain rather slow algebraic rates of convergence, whereas for $p_1 = p_2 = N$, we gain exponential convergence (spectral accuracy). The unknown Dirichlet values are easier to approximate than their Neumann counterparts (which have a stronger singularity). However, we are able to gain 13 and 12 digits of accuracy for each, respectively, in less than 0.15 s (averaged over 100 realizations—see §3avii for more timing results) for $N = p_1 = p_2 = 45$ which uses 180 basis functions.

(v) Relation to boundary integral methods and the Wiener–Hopf method

Here, we relate the unified transform to boundary integral methods by showing that, for this particular geometry, the global relation can be derived from taking the Fourier transform of a boundary integral equation (this is not true in general). This means that for this particular

problem, we can view the unified transform as a Fourier boundary integral method. In the case of posing the problem on the upper half plane as discussed above, and taking the limit of Green's representation formula from within the domain to the boundary, we obtain the integral equation

$$\int_{-\infty}^{\infty} G(x-y)g(y) dy + \frac{1}{2}h(x) = -\int_0^{\infty} G(x-y)f(y) dy, \quad (3.17)$$

where we have defined the functions

$$g(\tau) = \begin{cases} q_y(\tau), & \text{for } \tau < 0 \\ 0, & \text{otherwise} \end{cases} \quad h(\tau) = \begin{cases} q(\tau), & \text{for } \tau > 0 \\ 0, & \text{otherwise} \end{cases}$$

and G denotes a fundamental solution of the equation. Extending the function f to have the value zero along the negative real axis and taking Fourier transforms yields the equation

$$\hat{G}(\omega)\hat{g}(\omega) + \frac{1}{2}\hat{h}(\omega) = -\hat{G}(\omega)\hat{f}(\omega). \quad (3.18)$$

We have $G(x) = K_0(k_0|x|)/(2\pi)$, where K_0 is the modified Bessel function of the second kind of zeroth order, and the integral

$$\hat{G}(\omega) = \frac{1}{2\pi} \int_{-\infty}^{\infty} e^{i\omega x} K_0(k_0|x|) dx = \frac{1}{2} (k_0^2 + \omega^2)^{-1/2}. \quad (3.19)$$

The change of variables $\omega = (\lambda^{-1} - \lambda)\beta$ (where $\lambda \in \mathbb{R}_-$ so that $-(\lambda^{-1} + \lambda)\beta = \sqrt{k_0^2 + \omega^2}$) then yields the equation

$$\hat{g}[(\lambda^{-1} - \lambda)\beta] - (\lambda^{-1} + \lambda)\beta\hat{h}[(\lambda^{-1} - \lambda)\beta] = -\hat{f}[(\lambda^{-1} - \lambda)\beta], \quad (3.20)$$

which is equivalent to (3.7). Note also that (3.18) together with (3.19) is precisely the equation that appears (with complex ω) in the solution of the problem using the Wiener-Hopf method.

The unified transform has some desirable properties over the typical boundary integral methods posed in physical space. By choosing suitable basis functions, the unified transform avoids entirely the evaluation of singular integrals, emphasized by the above example where convolution becomes multiplication in Fourier space. There is a vast literature on effective quadratures for methods based on boundary integrals [30–32]. A common approach is to discretize the boundary into a large number of boundary elements which generally leads to only algebraic convergence [33]. For example, we found that we could only achieve an error (in the above sense) of around 10^{-5} for the unknown Dirichlet values using 2000 standard quadratic elements densely clustered near the singularity. A full comparison with such a boundary element method would take up too much space. However, we note that such slow algebraic convergence will not be able to compete with the spectral convergence observed in figure 1. We also subtracted off the logarithmic singularity of the integrand for accurate quadrature and evaluated this separate part analytically. There are of course hp -versions of boundary element methods [34–36] which fare better. A much better class of methods for this particular problem are (pseudo-)spectral methods which we discuss next.

(vi) Comparison of spectral methods

The simplicity of the geometry of the problem opens up the possibility of the use of (pseudo-)spectral methods. For an introduction and history of these methods, we refer the reader to [37–39] and in particular [25,40] for a discussion of unbounded domains. In this section, we solve the problem (posed on the upper half plane) using such a method and also separation of variables. These methods are then compared to the unified transform when we discuss solving the problem for large k_0 .

The first step is to get rid of the singularities. The easiest way to do this is to define the complex variable $z = x + iy$ and deform the domain via $z \rightarrow z^{1/2}$. In the new coordinates, also denoted by

(x, y) , this transforms the problem to the quarter plane $x > 0, y > 0$ and

$$\frac{\partial^2 q}{\partial x^2} + \frac{\partial^2 q}{\partial y^2} - 4k_0^2(x^2 + y^2)q = 0, \quad (3.21)$$

subject to

$$\frac{\partial q}{\partial y}(x, 0) = 2xe^{-x^2/2} \quad x > 0, \quad q(0, y) = 0 \quad y > 0. \quad (3.22)$$

The above problem can be solved via separation of variables which leads to Weber's equation and the expansion

$$q(x, y) = \sum_{n=0}^{\infty} a_n \psi_{2n+1}(\sqrt{2k_0}x) F_n(2\sqrt{k_0}y). \quad (3.23)$$

Here ψ_m denotes the standard Hermite functions, whereas F_n denotes the rescaled parabolic cylinder function

$$F_n(z) = 2^n n! D_{-(2+2n)}(z). \quad (3.24)$$

Both of these (as well as their derivatives) have well-known recursion relations for quick and accurate computation. The boundary condition then enforces

$$\sum_{n=0}^{\infty} a_n \psi_{2n+1}(\tau) = -\frac{\tau}{k_0 \sqrt{\pi}} e^{-\tau^2/4k_0}. \quad (3.25)$$

This expansion highlights the difference in scales already mentioned when $k_0 \neq 1/2$. To approximately solve (3.25), we truncated the expansion to N terms and collocated at the (non-negative) zeros of $\psi_{2N+1}(\sqrt{2k_0}\cdot)$.

The above problem also suggests the approximate expansion

$$q(x, y) = \sum_{n=0}^{N-1} \sum_{m=0}^{M-1} a_{n,m} \psi_{2n+1}(l_1 x) \phi_m(l_2 y). \quad (3.26)$$

Here, we define

$$\phi_m(z) = e^{-z^2/2} Q_m(z), \quad (3.27)$$

where $\{Q_m\}_{m=0}^{\infty}$ are (normalized) orthogonal polynomials on the *half-line* with weight $w(z) = e^{-z^2}$. This choice is natural given the expected decay of the solution (also confirmed by the asymptotics of the F_n) and we choose $l_1 = l_2 = \sqrt{2k_0}$. There is no closed form expression for the coefficients used in the recursion relations defining $\{Q_m\}_{m=0}^{\infty}$. We follow [41] and compute these coefficients with high precision (this can be done very quickly in Matlab) recursively. From these, ϕ_m and their derivatives can be computed quickly and accurately. The zeros of ϕ_m can also be computed via diagonalizing a standard *symmetric* tridiagonal matrix using the computed coefficients (see [41] and electronic supplementary material for further details). These polynomials have recently appeared in the solution of kinetic equations via spectral methods [42,43]. To approximately solve (3.25), we took the expansion (3.26) and substituted it into equation (3.21). We evaluated at the tensor product grid formed by the zeros of $\psi_{2N+1}(\sqrt{2k_0}\cdot)$ and $\phi_M(\sqrt{2k_0}\cdot)$ yielding a system of equations for the unknown coefficients. These were supplemented by evaluating the boundary condition at $y = 0$ at the zeros of $\psi_{2N+1}(\sqrt{2k_0}\cdot)$, leading to an overdetermined system which we solved in the least-squares sense.

Figure 2 plots the first few functions ϕ_m and F_m . It also shows the convergence of separation of variables and the spectral method (choosing $M = N$) for the above discrete measures of error. Errors were computed in the original coordinate system (i.e. before applying the transformation $z \rightarrow z^{1/2}$). Both methods converge exponentially with very similar errors. We found the spectral method to converge much faster than other choices of basis functions such as Laguerre functions or Hermite functions in the y direction. The errors obtained by these methods are about an order of magnitude smaller than that of the unified transform for the same number of expansion functions

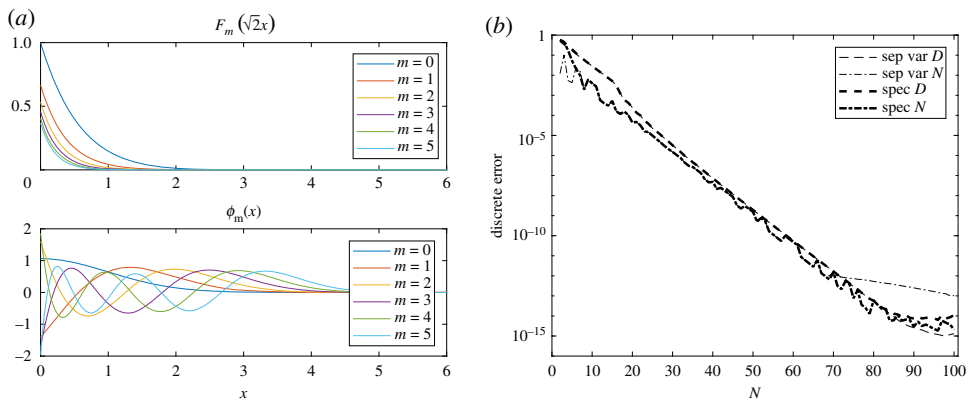


Figure 2. (a) Examples of the (rescaled) parabolic cylinder function and the orthogonal polynomials with an exponential weighting factor. (b) Convergence of the spectral method and separation of variables for this problem. D stands for Dirichlet values, whereas N stands for Neumann values. (Online version in colour.)

along the boundary (approximately 90). However, the spectral method/separation of variables become difficult to implement in more complicated geometries and it is not always possible to transform away the singularities. The unified transform copes with both of these problems and, as we shall see next, is faster to implement than the spectral method due to the fact that one only needs to expand functions along the *boundary*. Also, as will be discussed later, it fares better for large k_0 . However, an advantage of the above spectral method is that it automatically approximates the solution in the interior of the domain. For the unified transform, it is necessary to use Green’s representation formula to compute values in the interior using the boundary values. This is explored in [11] for *bounded* domains. Future work will focus on extending this efficiently to unbounded domains.

(vii) High frequency

We now compare the unified transform to the above spectral method and separation of variables for the case of large k_0 , taking $M = k_0(2N + p_1 + p_2)/2$ collocation points for the unified transform. Figure 3 shows the size of the parameter N needed to gain an error of 0.01 (two digits) in the computed Dirichlet values as we vary k_0 . Here, N is the number of expansion functions along each side (which is double the previous N for the unified transform owing to the singular functions). We have measured the discrete (relative) error as before but now over 1000 equally spaced points from 0 up to the point past the peak at which the true solution reaches 0.1 of its maximum value. We also show the times taken for each such N (averaged over 100 runs) where we have excluded the time needed to compute the zeros of the expansion function (collocation points) for the spectral method and separation of variables. We see roughly linear growth in N with the frequency k_0 (this is known as the pollution effect in the boundary integral method literature [44]), but the unified transform needs far fewer basis functions to achieve the accuracy for larger k_0 . The same plot for the unified transform is also shown but with the requirement of four digits of accuracy which still requires fewer basis functions than the other methods. This can be explained by the two different natural decay rates in the solution: the unified transform is boundary-based so can easily capture these two rates via different scalings of the basis functions along each side. This is not possible for separation of variables and is extremely hard for spectral methods which would require the treatment of a boundary layer. Note also that the time taken for the unified transform is much less than the spectral method and even less than the separation of variables. This is partly due to the smaller N required, but also as the spectral method uses $\mathcal{O}(N^2)$ basis functions owing to the basis functions in the y -direction that expand the solution over the whole domain.

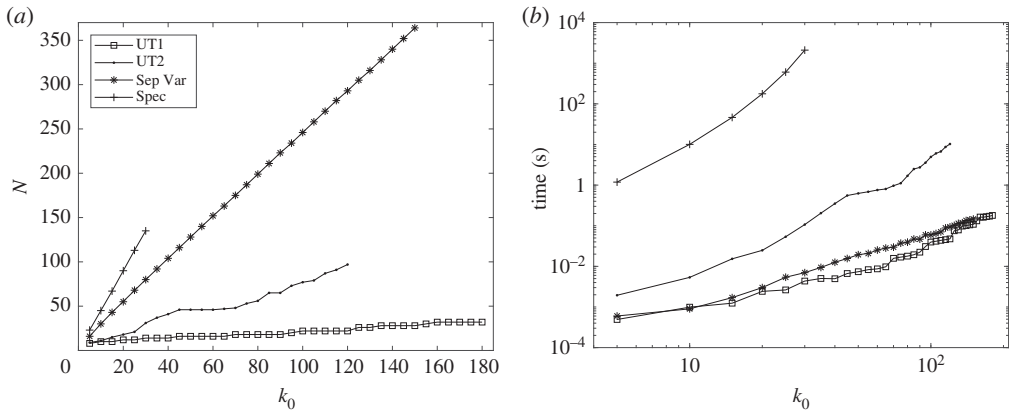


Figure 3. (a) Size of N along the boundary needed to gain the relevant accuracy. UT1 refers to two digits, whereas UT2 refers to four. Note that the number of basis functions for the spectral methods is actually N^2 . (b) The time taken for the methods.

From our results, it is apparent that the unified transform is more competitive than spectral methods for this problem due to the fact it is a boundary method, and can even compete with separation of variables due to the freedom in choosing appropriate basis functions.

(b) Helmholtz: two staggered finite parallel flat plates

We now consider the problem of acoustic scattering by two staggered parallel flat plates of the same finite length (lengths are non-dimensionalized by this), lying in $y=0, x \in [-a, 1-a]$ and $y=-h, x \in [0, 1]$, for some $a, h > 0$. The scattered field is found by solving the Helmholtz equation,

$$\frac{\partial^2 q}{\partial x^2} + \frac{\partial^2 q}{\partial y^2} + k_0^2 q = 0, \quad (3.28)$$

subject to

$$\frac{\partial q}{\partial y}(x, 0_{\pm}) = f(x), \quad x \in [-a, -a+1], \quad (3.29a)$$

$$[q](x, 0) = [q_y](x, 0) = 0, \quad x < -a, x > -a+1, \quad (3.29b)$$

$$\frac{\partial q}{\partial y}(x, -h_{\pm}) = g(x), \quad x \in [0, 1] \quad (3.29c)$$

and
$$[q](x, -h) = [q_y](x, -h) = 0, \quad x < 0, x > 1, \quad (3.29d)$$

where $f(x)$ and $g(x)$ are such that the total normal derivative on the plates is zero for a given incident field. We also impose the Sommerfeld radiation condition on the (full complex) solution.

To employ the unified transform, we consider three separate semi-infinite domains:

$$\mathcal{D}_1 = \{-\infty < x < \infty, 0_+ \leq y < \infty\}, \quad (3.30a)$$

$$\mathcal{D}_2 = \{-\infty < x < \infty, -\infty < y \leq -h_-\}, \quad (3.30b)$$

and
$$\mathcal{D}_3 = \{-\infty < x < \infty, -h_+ \leq y \leq 0_-\}. \quad (3.30c)$$

Evaluating the global relation (2.9) in the domains $\mathcal{D}_{1,2,3}$ and applying the normal derivative boundary conditions, yields the following three relations. Namely, from integrating along $\partial\mathcal{D}_1$, we obtain the relation

$$\begin{aligned} & \int_{-\infty}^{-a} e^{-i\beta x(\lambda+1/\lambda)} \left[-q_y(x, 0_+) + \beta \left(\lambda - \frac{1}{\lambda} \right) q(x, 0_+) \right] dx \\ & + \int_{-a}^{1-a} e^{-i\beta x(\lambda+1/\lambda)} \left[-f(x) + \beta \left(\lambda - \frac{1}{\lambda} \right) q(x, 0_+) \right] dx \\ & + \int_{1-a}^{\infty} e^{-i\beta x(\lambda+1/\lambda)} \left[-q_y(x, 0_+) + \beta \left(\lambda - \frac{1}{\lambda} \right) q(x, 0_+) \right] dx = 0, \end{aligned} \quad (3.31)$$

valid for $\lambda \in (-\infty, -1) \cup (0, 1) \cup \{e^{i\theta} : 0 < \theta < \pi\} = \Lambda_1$. Similarly, from integrating along $\partial\mathcal{D}_2$, we obtain the relation

$$\begin{aligned} & \int_{-\infty}^0 e^{-i\beta x(\lambda+1/\lambda)} \left[q_y(x, -h_-) - \beta \left(\lambda - \frac{1}{\lambda} \right) q(x, -h_-) \right] dx \\ & + \int_0^1 e^{-i\beta x(\lambda+1/\lambda)} \left[g(x) - \beta \left(\lambda - \frac{1}{\lambda} \right) q(x, -h_-) \right] dx \\ & + \int_1^{\infty} e^{-i\beta x(\lambda+1/\lambda)} \left[q_y(x, -h_-) - \beta \left(\lambda - \frac{1}{\lambda} \right) q(x, -h_-) \right] dx = 0, \end{aligned} \quad (3.32)$$

valid for $\lambda \in (-1, 0) \cup (1, \infty) \cup \{e^{i\theta} : \pi < \theta < 2\pi\} = \Lambda_2$. Finally, from integrating along $\partial\mathcal{D}_3$, we obtain

$$\begin{aligned} & e^{-\beta h(\lambda-1/\lambda)} \int_{-\infty}^0 e^{-i\beta x(\lambda+1/\lambda)} \left[-q_y(x, -h_+) + \beta \left(\lambda - \frac{1}{\lambda} \right) q(x, -h_+) \right] dx \\ & + e^{-\beta h(\lambda-1/\lambda)} \int_0^1 e^{-i\beta x(\lambda+1/\lambda)} \left[-g(x) + \beta \left(\lambda - \frac{1}{\lambda} \right) q(x, -h_+) \right] dx \\ & + e^{-\beta h(\lambda-1/\lambda)} \int_1^{\infty} e^{-i\beta x(\lambda+1/\lambda)} \left[-q_y(x, -h_+) + \beta \left(\lambda - \frac{1}{\lambda} \right) q(x, -h_+) \right] dx \\ & + \int_{-\infty}^{-a} e^{-i\beta x(\lambda+1/\lambda)} \left[q_y(x, 0_-) - \beta \left(\lambda - \frac{1}{\lambda} \right) q(x, 0_-) \right] dx \\ & + \int_{-a}^{1-a} e^{-i\beta x(\lambda+1/\lambda)} \left[f(x) - \beta \left(\lambda - \frac{1}{\lambda} \right) q(x, 0_-) \right] dx \\ & + \int_{1-a}^{\infty} e^{-i\beta x(\lambda+1/\lambda)} \left[q_y(x, 0_-) - \beta \left(\lambda - \frac{1}{\lambda} \right) q(x, 0_-) \right] dx = 0, \end{aligned} \quad (3.33)$$

valid for $\lambda \in \mathbb{R} \setminus \{0\} \cup \{e^{i\theta} : \theta \in [0, 2\pi]\}$.

We manipulate (3.31), (3.32) and (3.33) using the symmetry transform, defined now by $\lambda \rightarrow \lambda^{-1}$, to obtain two global relations. The first global relation arises from summing (3.32) multiplied by $e^{-\beta h(\lambda-1/\lambda)}$ with (3.33) and then subtracting the symmetry transform of (3.31), yielding

$$\begin{aligned} & \int_{-\infty}^{-a} e^{-i\beta x(\lambda+1/\lambda)} q_y(x, 0) dx + \int_{1-a}^{\infty} e^{-i\beta x(\lambda+1/\lambda)} q_y(x, 0) dx \\ & + \int_{-a}^{1-a} e^{-i\beta x(\lambda+1/\lambda)} \left[f(x) + \frac{\beta}{2} \left(\lambda - \frac{1}{\lambda} \right) [q](x, 0) \right] dx \\ & + e^{-\beta h(\lambda-1/\lambda)} \int_0^1 e^{-i\beta x(\lambda+1/\lambda)} \frac{\beta}{2} \left(\lambda - \frac{1}{\lambda} \right) [q](x, -h) dx = 0, \quad \lambda \in \Lambda_2. \end{aligned} \quad (3.34)$$

The second global relation arises from summing (3.31) with (3.33) and then subtracting $e^{-\beta h(\lambda-1/\lambda)}$ multiplied by the symmetry transform of (3.31), yielding

$$\begin{aligned} & \int_{-\infty}^0 e^{-i\beta x(\lambda+1/\lambda)} q_y(x, -h) dx + \int_1^{\infty} e^{-i\beta x(\lambda+1/\lambda)} q_y(x, -h) dx \\ & + \int_0^1 e^{-i\beta x(\lambda+1/\lambda)} \left[g(x) - \frac{\beta}{2} \left(\lambda - \frac{1}{\lambda} \right) [q](x, -h) \right] dx \\ & - e^{\beta h(\lambda-1/\lambda)} \int_{-a}^{1-a} e^{-i\beta x(\lambda+1/\lambda)} \frac{\beta}{2} \left(\lambda - \frac{1}{\lambda} \right) [q](x, 0) dx = 0, \quad \lambda \in \Lambda_1. \end{aligned} \quad (3.35)$$

Using simple transformations of integral variables, we transform each finite integral to $t \in [-1, 1]$, and each semi-infinite integral to $t \in [0, \infty)$. For our test problem, the transforms of f and g can be written down explicitly and we use the following expansions for the unknowns:

$$q_y(-t, -h) = \sum_{n=0}^{N_1-1} a_n S_{n,1}(t), \quad t > 0, \quad q_y(t+1, -h) = \sum_{n=0}^{N_2-1} b_n S_{n,2}(t), \quad t > 0, \quad (3.36a)$$

$$q_y(-t-a, 0) = \sum_{n=0}^{N_3-1} c_n S_{n,3}(t), \quad t > 0, \quad q_y(t+1-a, 0) = \sum_{n=0}^{N_4-1} d_n S_{n,4}(t), \quad t > 0, \quad (3.36b)$$

$$[q] \left(\frac{t+1}{2}, -h \right) = \sum_{n=0}^{N_5-1} e_n S_{n,5}(t), \quad t \in [-1, 1], \quad (3.36c)$$

and
$$[q] \left(\frac{t+1}{2} - a, 0 \right) = \sum_{n=0}^{N_6-1} f_n S_{n,6}(t), \quad t \in [-1, 1], \quad (3.36d)$$

for suitable expansion functions $\{S_{n,j}\}$. Substituting these expansions into (3.34) and (3.35) and evaluating at a finite number of allowed λ values gives a coupled linear system for the unknown coefficients.

(i) Basis choice and collocation points

For the finite intervals, to capture the $\sqrt{1-t^2}$ type singularity near the edge tips we define $\chi(t) = \arcsin(t) \in [-\pi/2, \pi/2]$ and the functions

$$C_m(t) = \begin{cases} \cos(m\chi(t)), & m \text{ odd} \\ i \sin(m\chi(t)), & m \text{ even} \end{cases}. \quad (3.37)$$

We used the basis functions $\{C_n(t)\}_{n=1}^N$ along each finite side which have the following Fourier transforms:

$$\int_{-1}^1 e^{i\lambda t} C_m(t) dt = -\frac{m\pi}{\lambda} J_m(-\lambda). \quad (3.38)$$

For the semi-infinite intervals, we used the Bessel functions $\{J_{(n+1)/2}(k_0 x)/x\}_{n=0}^{\tilde{N}-1}$. These have the advantage of capturing the correct singular behaviour near the plate edges when n is even. They decay with the correct algebraic rate at infinity and have Fourier transforms that are easy to compute [45]:

$$\int_0^{\infty} e^{i\lambda t} \frac{J_{\alpha}(bt)}{t} dt = \begin{cases} \frac{\exp(i\alpha \arcsin(\lambda/b))}{\alpha}, & \text{for } 0 \leq \lambda \leq b \\ \frac{b^{\alpha} \exp(\alpha\pi i/2)}{\alpha(\lambda + \sqrt{\lambda^2 - b^2})^{\alpha}}, & \text{for } 0 < b \leq \lambda \end{cases}. \quad (3.39)$$

For collocation points $\lambda \in \Lambda_1$, we chose M_1 Halton nodes in the interval $(0,1)$, minus their reciprocal values in $(-\infty, -1)$, and M_2 points in $\{e^{i\theta} : 0 < \theta < \pi\}$ with θ corresponding to Halton nodes in $(0, \pi)$. Reciprocal values were selected for $\lambda \in \Lambda_2$. With the change of variables $\omega = \beta(\lambda + \lambda^{-1})$, this corresponds to sampling frequencies along the entire real line of the Fourier

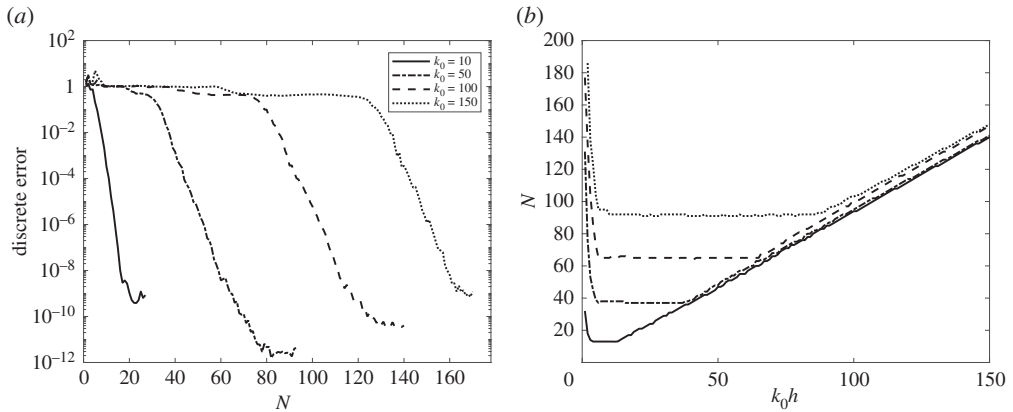


Figure 4. (a) Convergence of method for $h = 1$ and various k_0 . (b) Value of N needed to gain five digits of accuracy as we vary the parameter $k_0 h$.

transforms of the relevant functions. The complex collocation points along the unit circle are allowed precisely because the solution satisfies the Sommerfeld radiation condition so that the contribution of Green's identity along the relevant semi-circular arc vanishes in the infinite radius limit (see [13]). We found that to obtain accurate numerical solutions, we needed to sample these points and hence we considered the full complex solution. This corresponds to implementing the boundary conditions that make the boundary value problem well posed.

(ii) Numerical results

We consider a scattering problem with a plane wave incident at angle θ with the positive x -axis. This corresponds to the boundary functions

$$f(x) = ik_0 \sin(\theta) \exp[ixk_0 \cos(\theta)], \quad g(x) = ik_0 \sin(\theta) \exp[ixk_0 \cos(\theta) + i hk_0 \sin(\theta)]. \quad (3.40)$$

The corresponding matrix Wiener–Hopf equation for this problem gives rise to a 4×4 problem containing multiple exponential factors which do not decay in the upper or lower half planes (see electronic supplementary material). It is not known if there is a suitable method for the approximate factorization of this matrix.

Figure 4 shows the convergence of the method for a range of k_0 and $h = 1$. We took $a = 0.2$, $\hat{N} = 2N$, $\theta = \pi/6$ and similar results were found for other values of a and θ . We have measured the error by looking at 201 equally spaced points in the interval $[-1, 1]$, comparing to converged values at larger N , dividing by the maximum amplitude of the computed solutions and taking the maximum error of the computed $[q](x, 0)$ and $[q](x, h)$. For collocation parameters, we took $M_1 = 6\hat{N}$ and $M_2 = 3\hat{N}$. The method appears to converge exponentially, largely following the convergence of the true expansion in the functions $\{C_m\}_{m \in \mathbb{N}}$. As expected, convergence is slower for larger k_0 . We have also shown the value of N required to gain five digits of accuracy in the solution as a function of the dimensionless parameter $k_0 h$ and for different k_0 . The results show that the method is able to gain accurate solutions over a wide range of parameters. However, convergence is slower for very small and very large $k_0 h$, as expected due to the more complicated solution. We found the effect of smaller h to be less severe for a closer to 0 (when the plates are exactly aligned). We have also shown typical solutions in figure 5.

(iii) Single-plate problem and comparison with a boundary integral method

To validate our numerical implementation, we have computed the solutions for the single-plate problem with a single-finite plate lying in the region $x \in [-\frac{1}{2}, \frac{1}{2}]$, $y = 0$. The single-plate solution can be obtained analytically in terms of Mathieu functions through the use of an elliptic

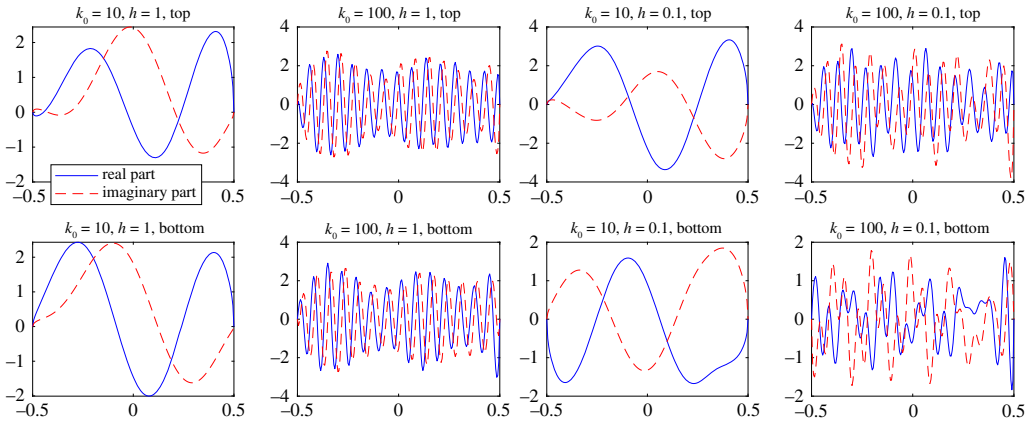


Figure 5. Typical ‘converged’ solutions for $h = 1$ and $h = 0.1$ and various k_0 . These were computed for $a = 0.2$ and $\theta = \pi/6$. (Online version in colour.)

coordinate system, discussed in [46] and briefly reviewed in the supplementary material. In what follows, we have computed a ‘converged’ reference solution using this expansion to measure errors. The global relation for this (easier) problem is given by (3.34) without the term involving the Fourier transform of $[q](x, -h)$.

We compare to a boundary integral method based on the work of Achenbach & Li [47] and recently improved in [48]. Other ways to treat boundary integral equations in cracked domains can be found in [49,50]. The single-plate problem is odd in the y variable and hence we can consider the problem in the upper half plane. Choosing the Green’s function that satisfies a homogeneous Dirichlet boundary condition on the x -axis, the boundary integral equations give rise to the following Fredholm integral equation of the first kind

$$ik_0 \sin(\theta) e^{ik_0 x \cos(\theta)} = -\frac{\partial}{\partial y} \int_{-1/2}^{1/2} q(x', 0_+) \frac{\partial G}{\partial y'}(x, 0; x', 0) dx', \quad (3.41)$$

where

$$G(x, y; x', y') = \frac{H_0^{(1)}\left(k_0 \sqrt{(x-x')^2 + (y-y')^2}\right)}{4i} - \frac{H_0^{(1)}\left(k_0 \sqrt{(x-x')^2 + (y+y')^2}\right)}{4i}. \quad (3.42)$$

The idea is to expand the unknown function

$$q(x, 0_+) = \sum_{m=1}^{\infty} a_m C_m(2x) \quad (3.43)$$

for which (3.41) gives rise to an infinite symmetric linear system for the unknown coefficients:

$$\sum_{m=1}^{\infty} \int_{-\infty}^{\infty} \frac{\sqrt{t^2 - 1}}{t^2} J_n(k_0 t/2) J_m(k_0 t/2) dt m a_m = -i \tan(\theta) J_n(\cos(\theta) k_0/2). \quad (3.44)$$

The difficult part of this method is the computation of the integrals of products of Bessel functions and we use the methods of [48]. We also mention that this is a similar approach to the method in [51] which seeks to solve singular integral equations by expanding the unknowns in a basis and solve the boundary integral equations as an infinite dimensional linear system using low rank approximations for sparse representations of the bivariate kernels.

Figure 6 shows the results for the unified transform and the above boundary integral method for $\theta = \pi/6$. The unified transform is able to gain near machine precision for a wide range of wavenumbers k_0 (the required number N to gain a specified number of digits also appears to

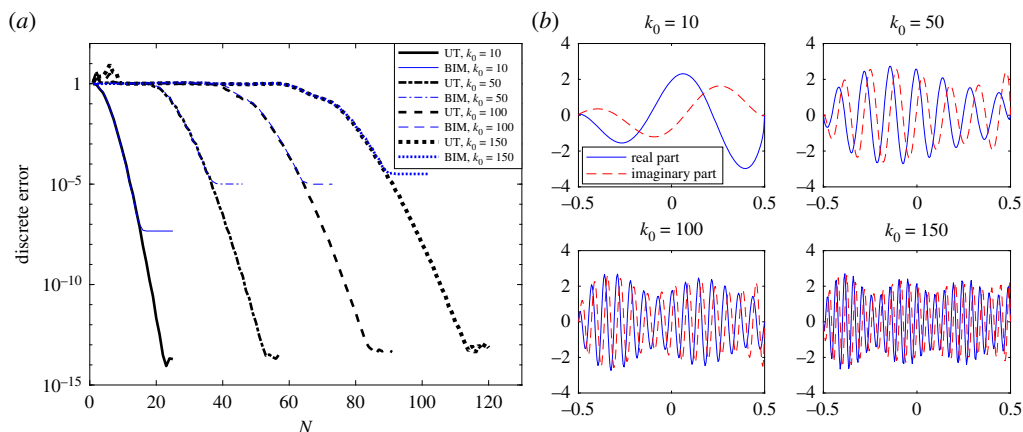


Figure 6. (a) Errors for the single-plate problem. UT denotes the unified transform, whereas BIM denotes the boundary integral method. (b) The analytic solutions $[q](x, 0)$ for different k_0 . (Online version in colour.)

grow sub-linearly with k_0), whereas the boundary integral method struggles, especially for larger wavenumbers. This is due to the difficulty in computing the integrals in (3.44), a difficulty which is entirely avoided when using the unified transform. Again the unified transform is very fast, taking a couple of seconds for $N = 120$ (600 basis functions), with the two plate problems only slightly slower.

4. Conclusion

In this paper, we use a new approach to solve mixed boundary condition problems usually considered via the Wiener–data values allows one to obtain an approximation for the unknown boundary values in a fast and accurate manner. This is the case even in situations where an approximate Wiener–Hopf solution is very difficult to obtain, such as matrix problems arising from multiple points at which the type of boundary condition changes. This new method, illustrated for one-point and four-point problems with flat plates, can be adapted for any number of finite or semi-infinite plates (not necessarily parallel) which is a topic of interest from a tradition Wiener–Hopf approach [52,53] and a boundary element approach [54]. In addition to N plates, the problem of N finite slits is also possible, such as that arising from a diffraction grating.

This new approach is seen to be highly accurate for the classic one-point problem where the solution can be calculated analytically. When compared with typical boundary element methods, this new spectral approach has the clear advantage of avoiding the evaluation of singular integrals. When compared with other spectral methods, this new approach shows similar rates of convergence and accuracy but is faster to implement in the case of complicated geometries (such as four-point problems) and can deal with singularities which cannot always be transformed away. Another advantage of being a boundary basis is that it can easily treat solutions with different scales/decay rates without the need to model boundary layers. We also found that the method was faster and more accurate for large k_0 when compared with the other methods.

We have also discussed suitable basis functions to capture the relevant singularities/decay at infinity as well as having easily computable Fourier transforms. This was crucial in gaining the exponential convergence of the method. One further case merits mentioning which is that of a finite edge with root singularities different from that discussed in §3b. Experimentation suggests that Jacobi polynomials multiplied by their respective weight are a good choice in this case (whose Fourier transforms can be represented by the confluent hypergeometric function). The methods presented here open up the possibility of using the unified transform for studying more general

exterior problems with a suitable decomposition of the unbounded domain. Future work will also aim at extending the method to three-dimensional problems.

Data accessibility. This work does not contain any original experimental data, and all of the results can be generated from the equations provided in the paper. However, relevant code for the numerical examples can be found at the first author's website: <http://www.damtp.cam.ac.uk/user/mjc249/code.html>.

Authors' contributions. M.J.C. produced and analysed the numerical method and results. M.J.C. and L.J.A. derived the mathematical model and its solution. All authors contributed to the writing of the manuscript and gave final approval for publication.

Competing interests. We declare we have no competing interests.

Funding. This work was supported by EPSRC grant EP/L016516/1 (M.J.C.), EPSRC Early-Career Fellowship EP/P015980/1 (L.J.A.) and EPSRC Senior Fellowship EP/RG8/609 (A.S.F.).

Acknowledgements. We thank two anonymous referees for their useful suggestions that led to the improvement of this paper. M.J.C. would also like to thank Bengt Fornberg and Sheehan Olver for discussions during the completion of this work.

References

1. Ursescu A, Eckart W, Marschall H, Hutter K. 2004 Inhomogeneous electric field generated by two long electrodes placed along parallel infinite walls separating different dielectric media. *J. Eng. Math.* **49**, 57–75. (doi:10.1023/B:ENGI.0000014892.85496.a6)
2. Noble B. 1988 *Methods based on the Wiener-Hopf technique for the solution of partial differential equations*. New York, NY: Chelsea Publishing Company.
3. Crighton DG, Dowling AP, Ffowcs Williams JE, Heckl M, Leppington FG. 1992 Modern methods in analytical acoustics: lectures notes. *J. Acoust. Soc. Am.* **92**, 3023. (doi:10.1121/1.404334)
4. Abrahams ID, Wickham GR. 1988 On the scattering of sound by two semi-infinite parallel staggered plates. I. Explicit matrix Wiener–Hopf factorization. *Proc. R. Soc. A* **420**, 131–156. (doi:10.1098/rspa.1988.0121)
5. Kisil AV. 2016 Approximate Wiener–Hopf factorisation with stability analysis. PhD thesis, University of Cambridge.
6. Kisil A, Ayton LJ. 2018 Aerodynamic noise generated by finite porous extensions to rigid trailing edges. *J. Fluid. Mech.* **836**, 117–144. (doi:10.1017/jfm.2017.782)
7. Fokas AS. 2008 *A unified approach to boundary value problems*. Philadelphia, PA: SIAM.
8. Sifalakis AG, Fokas AS, Fulton SR, Saridakis YG. 2008 The generalized Dirichlet–Neumann map for linear elliptic PDEs and its numerical implementation. *J. Comput. Appl. Math.* **219**, 9–34. (doi:10.1016/j.cam.2007.07.012)
9. Crowdy DG, Luca E. 2014 Solving Wiener–Hopf problems without kernel factorization. *Proc. R. Soc. A* **470**, 20140304. (doi:10.1098/rspa.2014.0304)
10. Hashemzadeh P, Fokas AS, Smitheman SA. 2015 A numerical technique for linear elliptic partial differential equations in polygonal domains. *Proc. R. Soc. A* **471**, 20140747. (doi:10.1098/rspa.2014.0747)
11. Colbrook MJ, Hashemzadeh P, Fokas AS. A hybrid analytical–numerical technique for elliptic PDEs. Preprint.
12. Ffowcs Williams JE, Hawkings DL. 1969 Sound generation by turbulence and surfaces in arbitrary motion. *Proc. R. Soc. A* **264**, 321–342. (doi:10.1098/rsta.1969.0031)
13. Spence EA. 2011 Boundary value problems for linear elliptic PDEs. PhD thesis, University of Cambridge.
14. Colbrook MJ, Flyer N, Fornberg B. 2018 On the Fokas method for the solution of elliptic problems in both convex and non-convex polygonal domains. *J. Comput. Phys.* **374**, 996–1016. (doi:10.1016/j.jcp.2018.08.005)
15. Crowdy D. 2015 Fourier–Mellin transforms for circular domains. *Comput. Methods Funct. Theory* **15**, 655–687. (doi:10.1007/s40315-015-0139-6)
16. Crowdy D. 2015 A transform method for Laplace's equation in multiply connected circular domains. *IMA J. Appl. Math.* **80**, 1902–1931. (doi:10.1093/imamat/hxv019)
17. Luca E, Crowdy D. 2018 A transform method for the biharmonic equation in multiply connected circular domains. *IMA J. Appl. Math.* **83**, 942–976. (doi:10.1093/imamat/hxy030)

18. Colbrook MJ. Extending the unified transform: curvilinear polygons and variable coefficient PDEs. <https://academic.oup.com/imajna/advance-article/doi/10.1093/imanum/dry085/5210368>.
19. Colbrook MJ, Fokas AS. 2018 Computing eigenvalues and eigenfunctions of the Laplacian for convex polygons. *Appl. Numer. Math.* **126**, 1–17. (doi:10.1016/j.apnum.2017.12.001)
20. Fornberg B, Flyer N. 2011 A numerical implementation of Fokas boundary integral approach: Laplace's equation on a polygonal domain. *Proc. R. Soc. A* **467**, 2983–3003. (doi:10.1098/rspa.2011.0032)
21. Li ZC, Lu TT. 2000 Singularities and treatments of elliptic boundary value problems. *Math. Comput. Model.* **31**, 97–145. (doi:10.1016/S0895-7177(00)00062-5)
22. Costabel M, Dauge M. 1993 Construction of corner singularities for Agmon-Douglis-Nirenberg elliptic systems. *Math. Nachr.* **162**, 209–237. (doi:10.1002/mana.19931620117)
23. Kozlov VA, Mazia VG, Rossmann J. 2001 *Spectral problems associated with corner singularities of solutions to elliptic equations*. Providence, RI: American Mathematical Society.
24. Kellogg RB. 1972 Higher order singularities for interface problems. In *The mathematical foundations of the finite element method with applications to partial differential equations* (Proc. Sympos., Univ. Maryland, Baltimore, MD, 1972), pp. 589–602. New York, NY: Academic Press.
25. Boyd J. 2001 *Chebyshev and Fourier spectral methods*. New York, NY: Dover Publications.
26. Niederreiter H. 1992 *Random number generation and quasi-Monte Carlo methods*. Philadelphia, PA: SIAM.
27. Tang T. 1993 The Hermite spectral method for Gaussian-type functions. *SIAM J. Sci. Comput.* **14**, 594–606. (doi:10.1137/0914038)
28. Boyd JP. 1984 Asymptotic coefficients of Hermite function series. *J. Comput. Phys.* **54**, 382–410. (doi:10.1016/0021-9991(84)90124-4)
29. Fornberg B, Merrill D. 1997 Comparison of finite difference-and pseudospectral methods for convective flow over a sphere. *Geophys. Res. Lett.* **24**, 3245–3248. (doi:10.1029/97GL03272)
30. Colton D, Kress R. 2013 *Integral equation methods in scattering theory*. Philadelphia, PA: SIAM.
31. Smith RNL. 2000 Direct Gauss quadrature formulae for logarithmic singularities on isoparametric elements. *Eng. Anal. Bound. Elem.* **24**, 161–167. (doi:10.1016/S0955-7997(99)00054-5)
32. Kolm P, Rokhlin V. 2001 Numerical quadratures for singular and hypersingular integrals. *Comput. Math. Appl.* **41**, 327–352. (doi:10.1016/S0898-1221(00)00277-7)
33. Unger G. 2009 *Analysis of boundary element methods for Laplacian eigenvalue problems*. Graz, Austria: Verlag der Technical University.
34. Babuška I, Guo BQ, Stephan EP. 1990 On the exponential convergence of the hp version for boundary element Galerkin methods on polygons. *Math. Method Appl. Sci.* **12**, 413–427. (doi:10.1002/(ISSN)1099-1476)
35. Stephan EP. 1996 The hp boundary element method for solving 2-and 3-dimensional problems. *Comput. Methods Appl. Mech. Eng.* **133**, 183–208. (doi:10.1016/0045-7825(95)00940-X)
36. Gwinner J, Stephan EP. 2018 Exponential convergence of hp-bem. In *Advanced boundary element methods*, pp. 269–294. Berlin, Germany: Springer.
37. Trefethen LN. 2000 *Spectral methods in MATLAB*. Philadelphia, PA: SIAM.
38. Fornberg B. 1996 *A practical guide to pseudospectral methods*. Cambridge, UK: Cambridge University Press.
39. Gottlieb D, Orszag SA. 1977 *Numerical analysis of spectral methods: theory and applications*. Philadelphia, PA: SIAM.
40. Shen J, Wang L-L. 2009 Some recent advances on spectral methods for unbounded domains. *J. Commun. Comput. Phys.* **5**, 195–241.
41. Shizgal B. 1981 A Gaussian quadrature procedure for use in the solution of the Boltzmann equation and related problems. *J. Comput. Phys.* **41**, 309–328. (doi:10.1016/0021-9991(81)90099-1)
42. Landreman M, Ernst DR. 2013 New velocity-space discretization for continuum kinetic calculations and Fokker-Planck collisions. *J. Comput. Phys.* **243**, 130–150. (doi:10.1016/j.jcp.2013.02.041)
43. Wilkening J, Cerfon AJ, Landreman M. 2015 Accurate spectral numerical schemes for kinetic equations with energy diffusion. *J. Comput. Phys.* **294**, 58–77. (doi:10.1016/j.jcp.2015.03.039)
44. Chandler-Wilde SN, Graham IG, Langdon S, Spence EA. 2012 Numerical-asymptotic boundary integral methods in high-frequency acoustic scattering. *Acta numerica* **21**, 89–305. (doi:10.1017/S0962492912000037)

45. Olver FWJ, Lozier DW, Boisvert RF, Clark CW. 2010 *NIST handbook of mathematical functions*. Cambridge, UK: Cambridge University Press.
46. McLachlan NW. 1964 *Theory and application of Mathieu functions*. New York, NY: Dover Publications.
47. Achenbach JD, Li ZL. 1986 Reflection and transmission of scalar waves by a periodic array of screens. *Wave motion* **8**, 225–234. (doi:10.1016/S0165-2125(86)80045-2)
48. Nigro D. 2017 Prediction of broadband aero and hydrodynamic noise: derivation of analytical models for low frequency. PhD thesis, University of Manchester.
49. Portela A, Aliabadi MH, Rooke DP. 1992 The dual boundary element method: effective implementation for crack problems. *Int. J. Numer. Meth. Eng.* **33**, 1269–1287. (doi:10.1002/(ISSN)1097-0207)
50. Cruse TA. 2012 *Boundary element analysis in computational fracture mechanics*. Dordrecht, The Netherlands: Kluwer Academic Publishers.
51. Slevinsky RM, Olver S. 2017 A fast and well-conditioned spectral method for singular integral equations. *J. Comput. Phys.* **332**, 290–315. (doi:10.1016/j.jcp.2016.12.009)
52. Brannan JR, Ervin VJ, Duan J, Razoumov L. 2004 A Wiener-Hopf approximation technique for a multiple plate direction problem. *Math. Method Appl. Sci.* **27**, 19–34. (doi:10.1002/(ISSN)1099-1476)
53. Korolkov AI, Shanin AV. 2015 Diffraction by a grating consisting of absorbing screens of different height. *New equations. J. Math. Sci.* **206**, 270–287. (doi:10.1007/s10958-015-2311-y)
54. Hewett DP, Langdon S, Chandler-Wilde SN. 2015 A frequency-independent boundary element method for scattering by two-dimensional screens and apertures. *IMA J. Numer. Anal.* **35**, 1698–1728. (doi:10.1093/imanum/dru043)